Identification of the Uncertainty Structure to Estimate the Acoustic Release of Chemotherapeutics From Polymeric Micelles

Ali Wadi, Mamoun Abdel-Hafez, and Ghaleb A. Husseini

Abstract—This paper estimates the acoustic drug release from micelles after accurately identifying the underlying statistical noise characteristics in experimental data. The drug release is measured as a change in fluorescence as ultrasound is applied. First, the noise structure affecting the process dynamics and the measurement process is identified in terms of statistical covariance of the aforementioned quantities. Then, the identified covariance magnitudes are utilized to estimate the dynamics of drug release. The performance of different filters is investigated. The identified apriori knowledge is used to implement an optimal Kalman filter, a multi-hypothesis Kalman filter, and a variant of the full information estimator (moving horizon estimator) to the problem at hand. The proposed algorithms are initially deployed in a simulation environment, and then the experimental datasets are fed into the algorithms to validate their performance. Experiments span a number of ultrasonic power densities for both non-targeted and targeted polymeric micelles(the targeting being accomplished using the folate moiety). The results suggest that the proposed algorithm, the optimal Kalman filter, performs better than the other two in all tests performed.

IndexTerms—Chemotherapy, drug release, full information estimator, moving horizon estimator, Kalman filter, modeling, pluronic micelles, ultrasound.

I. Introduction

MANY cancers are treated using anti-neoplastic agents that usually target the fast growing property of these malignant tissues. Those chemicals are administered intravenously, and they circulate systemically until they reach the diseased location. Advances in nanotechnology have allowed for the spatial and temporal release of chemotherapeutics from nanocarriers upon reaching the cancerous site. These nanocarriers, including micelles and liposomes, are examples of the utility of nanotechnology in this area of medicine [1]. Our system specifically uses ultrasound as a trigger to release their contents. Several reports have demonstrated the mechanism by which ultrasound actuation stimulates the carriers to release their encapsulated agents [2]–[9].

Disturbances that plague dynamic systems not only degrade control performance, but also interfere with the dynamics of a given system as well as the measurement process. Those disturbances, which will be referred to as noise, affect both the dynamics and measurement models. Noise, in the dynamics of a system, represent uncertainty in the mathematical model as well as disturbances arising from the process itself. This type of noise gets propagated along with the state in the mathematical model to account for unmodeled dynamics. Noise in the measurement process represents disturbances and uncertainty attributed to the measurement apparatus. Knowledge of both types of noise is crucial in estimating the states of any system. Failure to properly account for noise will breach the optimality of an implemented estimator, and that will result in inaccurate estimates of the state of interest. Identifying the noise statistics associated with a given dynamic system is addressed in literature, and some of the methods that aim to characterize the statistics include Bayesian, Maximum Likelihood, Correlation, and Autocovariance Least-squares techniques [10]. Maximum Likelihood estimation is used here to identify the noise covariance magnitudes affecting the process.

The release of Doxorubicin (Dox) from Pluronic P105 (P105) micelles has been studied using both mechanistic and probabilistic models [11]–[13]. This work attempts to accurately predict the behavior of this drug delivery process through multiple stochastic and optimization-based approaches. The Kalman filter is a stochastic approach that fuses the dynamics and the measurements of the system to produce an estimate of the state of interest. Knowledge of the drug encapsulation dynamics system model, alongside the measurements undertaken, is used to obtain an optimal estimate of drug encapsulation. The Kalman filter is a minimum-mean square-error technique that minimizes the expected value of the square error between the estimate and the true value of the drug encapsulation (measured as a percent). The Moving Horizon estimator is an optimization-based maximum likelihood approach, which attempts to produce an estimate through finding the set of states that maximizes the probabilistic likelihood of that state based on measurements [14], [15]. Application of the aforementioned filters on our drug delivery system as well as the identification of the uncertainty structure in the system is a novel effort. It is worth mentioning, however, that an attempt to estimate the state of this drug delivery system using a variant of the Kalman filter is reported by Abdel-Hafez and Husseini [16].

In this work, the noise structure of the dynamics of our system is first identified through a maximum likelihood approach. Consequently, a number of estimators, which use the identified *a priori* information, are used to acquire an optimal estimate for the percent of the drug released. The proposed drug release estimation approach is crucial to designing a model-predictive

https://doi.org/10.1109/TNB.2017.2736021

controller for cancer treatment. A high-accuracy estimate of percent drug release is needed to enhance the optimality of the controller. Additionally, to control the treatment process, the predicted state of percent drug release is needed at times when measurements are not available. This is where the proposed high-accuracy percent drug release estimation method is vital.

II. Methods and Mathematical Model

A.Experimental Methods

The carrier, Pluronic® P105, is prepared when the polymeric micelles are dissolved in a phosphate buffered saline solution. The Pluronic® P105 solution is then used to dissolve Doxorubicin, at a concentration of $4.5\mu g/ml$ in 5% copolymer wt. concentration. Two Pluronic® P105 solutions are used; non-targeted as well as targeted (using the folate moiety as a target) ones. The exact details pertaining to how the drug delivery system is prepared are detailed in [16].

B.Measurement Technique

Since Dox release can be measured as a function of a change in fluorescence, a chamber was constructed to quantify this change upon the application of ultrasound. The chamber is in a thermostated bath that maintains a constant temperature of 37°C, simulating a physiologically relevant temperature. An argon ion laser emits a beam that gets split by a beam splitter attenuator into two portions. The first portion is directed to a photodetector that measures the power of the laser, while the other portion is directed into a fiber optic bundle. For an excitation wavelength of 488 *nm*, the concentration of Dox can be quantified through the measurement of fluorescence at 535 *nm*. The means to deliver and collect the emissions is a multimode fibre optic probe. A filter is used to cut off emissions/scattered light that is less than 517 *nm* in wavelength [15].

The percent ultrasonic release of Dox from the core of these micelles is related to the change in the fluorescence intensity of the environment surrounding Pluronic® P105 micelles as they release the Dox. This release results in a decrease in the measured fluorescence intensity because water molecules quench the fluorescence of our anti-neoplastic agent. The data are then normalized with respect to the intensity when full encapsulation of the drug is in effect. Since Dox is linear in concentration below a concentration of 15 μg, Equation 1 is used to calculate the percent release of the drug from these nanocarriers [16].

$$\%_{Release} = \frac{I_{P105} - I_{US}}{I_{P105} - I_{PBS}} \qquad (1)$$

where I_{P105} is the fluorescence intensity of the P105- encapsulated drug, I_{US} is the fluorescence intensity when sonication is in effect, I_{PBS} is the fluorescence intensity of the drug in the phosphate buffered saline solution, and the $\%_{Release} \in [0,1]$.

Ultrasound actuation to release the drug from the micelles is realized through a 70−kHz piezoelectric transducer embedded in an ultrasonicating bath. The frequency-modulated input waveform has a resolution of 0.12kHz. The manually driven ultrasound is applied every 10 seconds. When actuation stops, the fluorescence level rebounds to the original value (before ultrasound was turned on) suggesting that doxorubicin molecules are re-encapsulated back in the core of the micelles once the external stimulus (acoustic power) stops. It is of interest to indicate that the release on happens when ultrasound is applied [12], [17], [18].

C.Mechanistic Dynamic Model

The mathematical model describing the release and re-encapsulation processes used in this study is formulated by Husseini *et al.* [13]. It models the release of Dox from polymeric micelles to be of a constant rate when ultrasound is applied, and estimates the re-encapsulation as having firstorder kinetics with respect to the concentration of the free drug. The model implies that the application of ultrasound breaks down or disrupts the micelles at a rate that is constant and independent of micellar concentration. Consequently, the drug is released. As Dox leaves the micelles, free Dox molecules that are not taken up by the cancerous cells are re-encapsulated inside the micelles at a rate proportional to the concentration of the free drug. The drug can either be re-encapsulated inside micelles that were not destroyed, or into newly-formed nanocarriers.

The mathematical model is expressed as shown in equation (2), where E is the amount of drug encapsulated, F is the amount of free drug, T is the total amount of the drug in solution, k_r is the zero-order release rate constant, and k_e is the first order re-encapsulation rate constant.

$$E^{\cdot}|_{US} = -k_r + k_e F = -k_r + k_e (T - E) \qquad (2)$$

Numerous experiments were conducted with different ultrasonic power densities for both folate-targeted and non-targeted micelles. Folated-micelles target several cancer cell lines, including MCF7 (a breast cancer cell line). The experimental conditions and the corresponding re-encapsulation constants of the experiments are presented in Table I [13]. To elaborate on the nomenclature used, PF125 represents the use of Folated Pluronic P105 micelles at a variac setting of 125 V. This corresponds to

a power density of 3.54 W/cm^2, which are the conditions used to collect data for experiment 1. Similarly, POH135 represents the use of nonfolated Pluronic

TABLE I
EXPERIMENTAL CONDITIONS FOR CONDUCTED TESTS

Exp #		Micelless Type	Power Density (W/cm^2)	k_e
1	Folated Micelles	PF125	3.54	21.20
2		PF130	5.09	23.89
3		PF135	5.43	10.07
4		PF140	5.91	21.18
5	Non-Folated Micelles	POH125	3.54	27.38
6		POH130	5.09	26.41
7		POH135	5.43	31.86
8		POH140	5.91	23.16

P105 micelles at a variac setting of 135 V. This corresponds to a power density of 5.43 W/cm^2, which are the conditions used to collect data for experiment 7. The experimental conditions in Table I are then easily deciphered.

D. Data Acquisition

The release was acquired via the manual pulsation of the ultrasonic transduce housed in a sonicating bath. The fluorescence measurements as well as the imperfections in the inherent nature of the manual acoustic application resulted in a significantly noisy response. Multiple experiments were carried out, and multiple measurements were taken at different conditions. The kinetic constants of release, k_r, and encapsulation, k_e, that govern the dynamics of Equation 2 are derived in [13].

III. UNCERTAINTY AND ENCAPSULATION ESTIMATION

A. Uncertainty Structure Identification

The underlying uncertainty structure arise from two sources; a system dynamic noise coming from the process and a measurement noise coming from the measurement method/device. These two noise sequences are modeled to be zero-mean normal Gaussian white noise processes. The magnitudes of the process and measurement noise covariance processes are needed for optimal estimation of the percent drug encapsulation.

The model is discretized at a sampling frequency of 50 Hz, and it can be written as a dynamic equation and a measurement equation in linear state space form as shown in equations (3) and (4). E_K is the amount of drug encapsulated at time step k, u_K is the input between time steps k and k + 1, t is the sampling time period equal to 0.02 s, and w_k and v_{k+1} are the dynamics and measurement noises at times t_k and t_{k+1}.

$$\begin{aligned} E_{K+1} &= AE_k + u_k + w_k \\ &= \left(e^{-ke\Delta t}\right) E_k + (e^{-ke\Delta t} - 1) * \left(\frac{kr}{ke} - T\right) + w_k \quad (3) \\ z_{k+1} &= E_{K+1} + v_{k+1} \quad (4) \end{aligned}$$

Equation (3) is stable and the system represented in equations (3) and (4) is observable. The measurement equation can be written in terms of the drug encapsulation at time 0 as in equation (5):

$$\begin{bmatrix} z_0 \\ z_1 \\ \vdots \\ z_N \end{bmatrix} = \begin{bmatrix} A^0 \\ A^1 \\ \vdots \\ A^N \end{bmatrix} (E_0) + \begin{bmatrix} u_0 \\ u_1 \\ \vdots \\ u_N \end{bmatrix} + \begin{bmatrix} 0 & 0 & \dots & 0 \\ 1 & 0 & \dots & 0 \\ \vdots & \vdots & \ddots & \vdots \\ A^{N-1} & A^{N-2} & \dots & 1 \end{bmatrix} \begin{bmatrix} w_0 \\ w_1 \\ \vdots \\ w_N \end{bmatrix} + \begin{bmatrix} v_1 \\ v_2 \\ \vdots \\ v_{N+1} \end{bmatrix} \tag{5}$$

As the dynamics equation in (3) is stable, a less than unity in value, $\forall k > \tau$ time steps, $A^{\tau} < \delta$. where δ is a small threshold δ chosen to be less than $1x10^{-5}$. It is necessary for the value of δ to be small enough for subsequent time steps to be dominated in magnitude by the noises in the system. The chosen value for δ was one such that smaller values did not affect the solution of the solver used. Consequently, the measurements after τ time steps may be assumed to be independent of the initial state. This allows equation (5) to be rearranged as in equation (6). The vector Y contains measurements and inputs after time step τ and is seen to be a function of the dynamics and measurement noise sequences only.

$$\begin{aligned} Y &= \begin{bmatrix} z_\tau \\ z_{\tau+1} \\ \vdots \\ z_{N+\tau-1} \end{bmatrix} - \begin{bmatrix} 1 \\ 1 \\ \vdots \\ 1 \end{bmatrix} * (A-1)\left(\frac{kr}{ke} - T\right)\left(\sum_{j=0}^{\tau-1} A^j\right) \\ &\approx \begin{bmatrix} A^{\tau-1} & A^{\tau-2} & \dots & 1 & \dots & 0 \\ 0 & A^{\tau-1} & A^{\tau-2} & \dots & \dots & 0 \\ \vdots & \ddots & \vdots & \ddots & \vdots & \vdots \\ 0 & \dots & 0 & A^{\tau-1} & \dots & 1 \end{bmatrix} \begin{bmatrix} w_0 \\ w_1 \\ \vdots \\ w_{N+\tau-1} \end{bmatrix} \\ &\quad + \begin{bmatrix} v_\tau \\ v_{\tau+1} \\ \vdots \\ v_{N+\tau} \end{bmatrix} \end{aligned} \tag{6}$$

As a result of the normal distribution of the noise sequences, Y is a multivariate Gaussian distributed vector described as $Y \sim N(0, P)$ with covariance matrix P given by (7):

$$P = \Theta \begin{bmatrix} Q_w & & \\ & \ddots & \\ & & Q_w \end{bmatrix} \Theta^{\mathrm{T}} + \begin{bmatrix} R_v & & \\ & \ddots & \\ & & R_v \end{bmatrix} \tag{7}$$

where Q_w and R_v are the covariance magnitudes of the dynamics and measurement noises, respectively, the matrix multiplying the dynamic noise vector w in equation (6) is labeled as , and ^{T} is the transpose of .

The maximum likelihood estimation (MLE) problem is formulated by constructing the maximum likelihood equation of the multivariate normal distribution vector Y in equation (8) as:

$$\min_{Q_w, R_v} \left| \ln\left(|P|\right) + Y' * P^{-1} * Y \right| \qquad (8)$$

Therefore, the process and measurement covariance magnitudes, that minimize the MLE cost function in equation (8). represent the true statistics of the process and measurement noise sequences, denoted as Q_{MLE}, R_{MLE}, respectively. The estimate of the percent drug encapsulation is described next.

B. Encapsulation State Estimation

The encapsulated drug amount is calculated in percentage form as the difference between the total amount (100% encapsulated drug) and the released drug amount:

$$E\,(t) = 100\%_{Encapsulation} - \%\ release \qquad (9)$$

The identified process uncertainty structure from equation (8) allows for an optimal estimate of the percent drug encapsulation to be acquired using a Kalman filter approach. The approach starts with the initial conditions of the expected value of encapsulation given the measurement and its covariance presented below:

$$\begin{aligned} E\left[E_0|z_0\right] &= \hat{E}_0 \\ cov\left[E_0|z_0\right] &= P_0 \end{aligned} \qquad (10)$$

The state is propagated in time to get an *a priori* estimate, $\bar{E}_{K+1}$, using the dynamic model and an *a priori* state covariance, $\bar{P}_{K+1}$, given by:

$$\begin{aligned} \bar{E}_{\mathrm{K}+1} &= \hat{E}_{\mathrm{k}+1|\mathrm{k}} = A\hat{E}_{\mathrm{k}} + u_k \\ P_{K+1|k} &= \bar{P}_{K+1} = AP_kA + Q_{MLE} \end{aligned} \qquad (11)$$

The *a priori* measurement is then:

$$\mathrm{E}\left[z_{k+1|k}\right] = \bar{z}_{k+1} = \bar{E}_{\mathrm{K}+1} \qquad (12)$$

The innovation and the innovation covariance are defined as follows:

$$\begin{aligned} \tilde{z}_{k+1} &= z_{k+1} - \bar{z}_{k+1} \\ S_{k+1} &= \bar{P}_{K+1} + R_{MLE} \end{aligned} \qquad (13)$$

The optimal Kalman gain as well as the updated *a posteriori* state and covariance estimates are then shown to be:

$$W_{k+1} = \bar{P}_{K+1}\bar{S}_k^{+1}{}_1$$

$$\hat{E}_{\mathrm{k}+1} = \bar{E}_{\mathrm{K}+1} + W_{k+1}\tilde{z}_{k+1}$$

$$P_{k+1} = \bar{P}_{k+1} - W_{k+1}S_{k+1}W_k^T{}_{+1} \qquad (14)$$

The Kalman filter's estimate is optimal here; the identified covariance is representative of the statistics of the noise sequences, and no assumptions about these statistics were made. Therefore, this method is referred to as the Optimized Kalman filter.

To demonstrate the enhancement in the accuracy of the estimate of the drug encapsulation, in the next section, the proposed algorithm will be compared with two methods used in literature.

C.Comparison

The performance of the proposed algorithm will be compared with the two methods published in literature: the moving horizon estimator and the multiple model approach.

1)Moving Horizon Estimator (MHE): This method is an optimization technique applied to stochastic estimation. The benefit of the optimization structure is to utilize all available *a priori* information such as the bounds on the estimated states, knowledge of the feasible trajectory of the state and knowledge of the bounds of the disturbances [15], [19]. The technique is based on maximizing the conditional probability density function of the states given the measurements $p_{x|z}(x_k|z_k)$ to form a maximum likelihood problem. Starting with the aforementioned density, one can write:

$$
\begin{aligned}
& p_{E|z}(E_k|z_k) \\
&= \frac{\prod_0^T p_{z|E}(z_k|E_k) * p_E(E_k)}{\prod_0^T p_z(z_k)} \\
&= \frac{p_{E_o}(E_o) * \prod_0^T p_{z|E}(z_k|E_k) * p_{E|E}(E_{k+1}|E_k)}{\prod_0^T p_z(z_k)} \\
&= \frac{\prod_0^T p_v(z_k - E_k) * p_{E_o}(E_o) * \prod_0^T p_w(E_{k+1} - F(E_k, u_k, w_k))}{\prod_0^T p_z(z_k)} \\
&= \frac{\prod_0^T p_v(v_k) * p_{E_o}(E_o) * \prod_0^T p_w(w_k)}{c} \qquad (15)
\end{aligned}
$$

The resulting densities are those of the normally distributed noises $p_v(v_k)$, $p_w(w)$ and the density describing the distribution of the initial state, $p_{E0}(E_0)$. The statistical properties of the first two densities are known, but the last density is assumed to be normally distributed around a guess of the initial condition with state covariance equal to that of the predicted Kalman filter covariance. The above assumptions are valid in light of the considered linear system whose densities do not exhibit significant deviation from the Gaussian assumption. Taking the negative log of above conditional density, one obtains the maximum likelihood minimization problem shown in (16). The L^2 norm is defined as $\alpha^2_{\beta^{-1}} = \alpha'\beta^{-1}\alpha$.

$$
\min_{E_o, \{w\}_0^T, \{v\}_0^T} \left| \phi\left(E_o, \{w\}_0^T, \{v\}_0^T\right) \right| \qquad (16)
$$

where

$$
\begin{aligned}
& \phi\left(E_o, \{w\}_0^T, \{v\}_0^T\right) \\
&= p_{E_0}(E_o) + \sum_{k=0}^{T} -ln\left(p_v(v)\right) + \sum_{k=0}^{T} -ln\left(p_w(w)\right) \\
&= \left\| E_o - \bar{E}_o \right\|^2_{P^{-1}} + \sum_{k=0}^{T} \|v_k\|^2_{R^{-1}_{MLE}} + \sum_{k=0}^{T} \|w_k\|^2_{Q^{-1}_{MLE}}
\end{aligned}
$$

Equation (16) can be written as in equation (17). The first term in (17) costs deviations of the state from the initial guess, the second term costs deviations of the measurement from the predicted measurement, and the last term costs the magnitude of the dynamic noise vector. The optimization problem takes in the entire trajectory of the measurement and minimizes the cost function, φ, by choosing the initial state, E_o, as well as the entire dynamic process noise vector, $\{\boldsymbol{W}\}_0^T$. The state can then be reconstructed based on the output of the solver through equations (2-3). The MATLAB nonlinear solver, "fmincon", is used to solve the optimization problem.

$$\min_{E_o,\{w\}_o^T} \left|\varphi\left(E_o,\{w\}_0^T\right)\right| \tag{17}$$

where

$$\varphi\left(E_o,\{w\}_0^T\right) = \left\|E_o-\bar{E}_o\right\|_{P^{-1}}^2 + \sum_{k=0}^{T}\left\|z_k - F(E_k,u_k,w_k)\right\|_{R_{MLE}^{-1}}^2 + \sum_{k=0}^{T}\left\|w_k\right\|_{Q_{MLE}^{-1}}^2$$

The full information estimator is an offline post-processing tool. This is where the Moving Horizon Estimator comes into play; it is a full information estimator applied only to a window when a certain number of measurements have been logged [19]–[21]. This enables the problem to be solved online at the cost of losing some accuracy due to not utilizing the full trajectory of the state. The derivation of (15) changes for the initial state probability density function, which is called the arrival cost in the context of MHE. The arrival cost describes the prior information from the previous sequence of measurements. For the considered linear system with normally distributed density functions, the arrival cost, $Z_K(E_T)$, is given by (18), where $E\hat{}_{K-1}$ is the estimate of the previous time step and $P(K)$ is the covariance update recursion from the Kalman filter [22]–[24].

$$Z_K(E_T) = \left\|E_K - A\hat{E}_{K-1} - u_{K-1}\right\|_{P_k^{-1}}^2$$
$$P_k = AP_{k-1}A + Q - AP_{k-1}(P_{k-1}+R)^{-1}P_{k-1}A \tag{18}$$

The arrival cost penalizes deviations from the previously estimated state, which is assumed to best describe the preceding measurement window [25].

2)A Multiple Model Approach: This approach was devised in [16], and it was compared against a Kalman filter with guessed statistical noise characteristics. In this approach, several Kalman filters operate in parallel, and each filter operates with a hypothesized measurement noise covariance. On the other hand, the dynamics noise statistics are assumed to be known. Uncertainty in the ultrasound frequency, amplitude, time, pulse time, and distance from target are the reasons that motivated the use of this approach. Each assumption yields an estimate for the encapsulated drug state, and the final estimate is a probabilistic sum of the estimates of the Kalman filters. The process is detailed in [16], and it will not be derived here. However, the proposed method improves on the previous method in that both the covariance of the measurement noise and the covariance of the dynamics noise are estimated. This will realize the optimal property of the Kalman filter. Consequently, the filter will be stable with bounded errors in the estimated state.

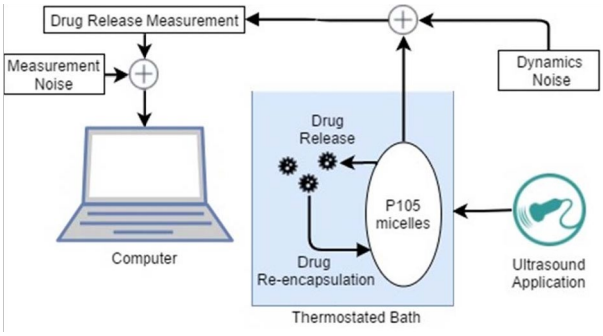

Fig. 1. Test bed schematic.

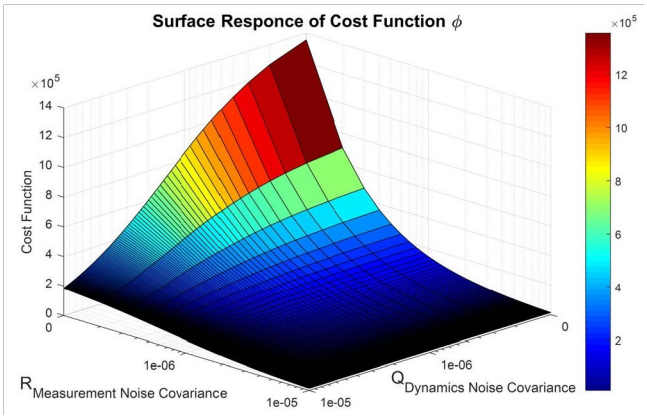

Fig. 2. Cost function variation with changing Q and R.

TABLE II
MLE IDENTIFIED DYNAMICS AND MEASUREMENT NOISE COVARIANCE VALUES FOR EXPERIMENTS 1, 2 AND 5

Covariance Type	Exp. 1	Exp. 2	Exp. 5
Dynamics noise covariance (Q_{MLE})	$8.14x10^{-3}$	$8.00x10^{-3}$	$1.70x10^{-4}$
Measurement noise covariance (R_{MLE})	$1.00x10^{-4}$	$1.00x10^{-4}$	$1.00x10^{-4}$

IV. RESULTS

A. Uncertainty Identification

The proposed MLE method was applied to the experiments shown in Table I to identify the statistics of the measurement and process noise sequences. The numerical solver in the MATLAB environment was used to identify the global minimum based on the constraints and limits imposed. The cost function was found to be smooth and convex under the aforementioned settings. For experiment 1, the surface response of the obtained MLE cost function is shown in figure 2.

From figure 2, it is evident through inspection of the surface response and by examining the solution that the constraints played a role in the obtained covariance values. The reason being that the minimizing solution of the measurement covariance value happens to be the lower bound. The minimizing solution takes the values documented in Table II.

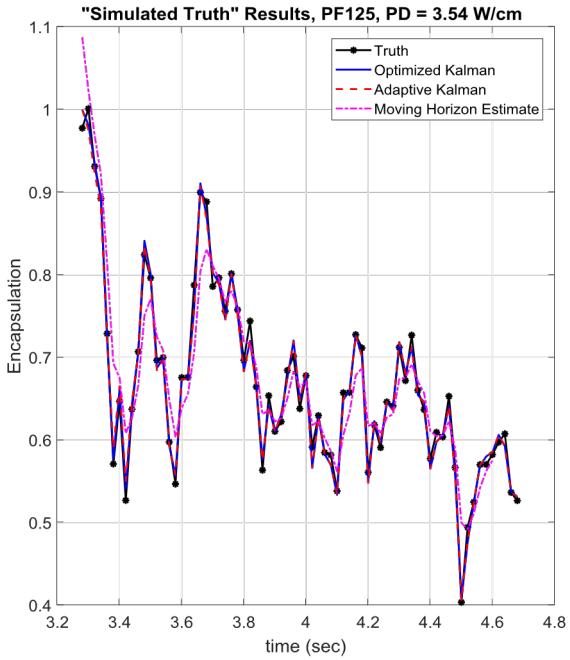

Fig. 3. Comparison of Estimators in simulated environment (Experiment 1).

TABLE III
ESTIMATION MEAN SQUARE ERROR IN SIMULATED ENVIRONMENTS

Estimator	MSE 1	MSE 2	MSE 5
MLE Optimized Kalman Filter	$3.50\text{x}10^{-3}$	$5.29\text{x}10^{-3}$	$1.70\text{x}10^{-3}$
Adaptive Kalman Filter	$3.56\text{x}10^{-1}$	$4.96\text{x}10^{-2}$	$2.50\text{x}10^{-3}$
Moving Horizon Estimator	$1.52\text{x}10^{-1}$	$4.23\text{x}10^{-1}$	$2.81\text{x}10^{-1}$

All the filters were fed an initial encapsulation state of $E_0 = 1$, and an initial encapsulation covariance of $P_0 = 1$. The Moving Horizon Estimator is free to deviate from the suggested initialization depending on the cost imposed by the initialization in the optimization problem. The filters employ the noise statistics presented in Table II.

B.Simulation Results

The algorithms were first tested in simulation. Equations 3 and 4 were used to simulate the dynamic as well as the measurement process of our system. The MLE optimized Kalman filter, the Moving Horizon Estimator as well as the adaptive Kalman filter, were used to estimate the drug encapsulation percent. The true state, which was simulated, is known in this case, and performance validation is possible. Figures 3, 4 and 5 present the encapsulation estimation results for the various estimators for two experimental conditions.

Figures 3, 4 and 5 show the simulated truth for encapsulation as well as the estimate of the filters. The MLE optimized Kalman filter seems to closely follow the truth; on the other hand, the adaptive Kalman and the MHE follow the general trend of the state trajectory. Table III quantitatively describes the performance of the filters through presenting the mean square error of 100 Monte-Carlo simulations for each filter. The numbers confirm the observations. They suggest

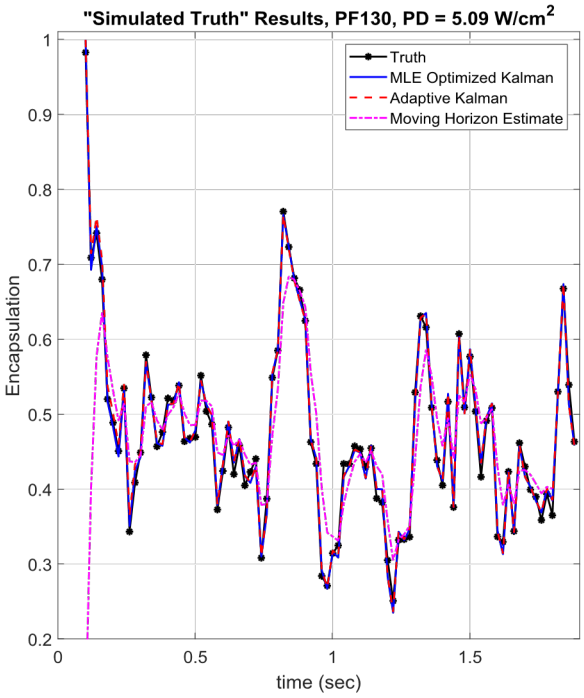

Fig. 4. Comparison of Estimators in simulated environment

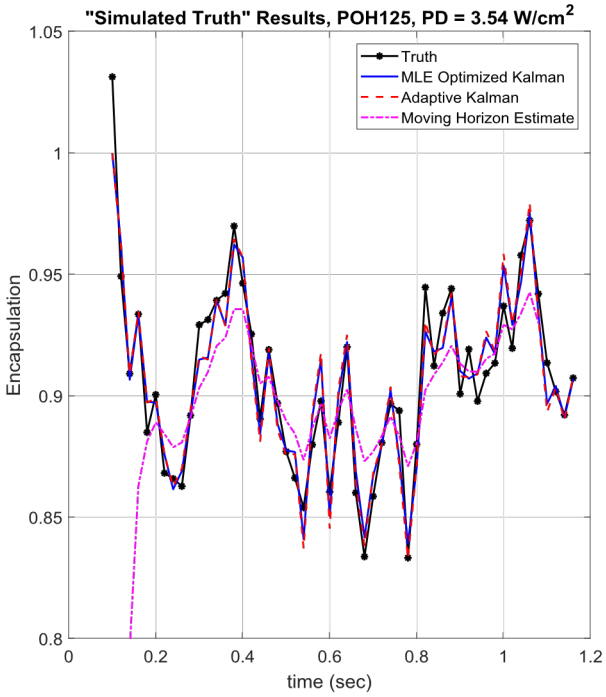

Fig. 5. Comparison of Estimators in simulated environment (Experiment 5).

that the MLE optimized Kalman filter outperforms the other algorithms. The reason behind the difference can be attributed to the fact that the correct information for the statistics of both the dynamics noise and the measurement noise are available from the start in the optimal filter. This is contrary to the fact that the adaptive Kalman filter assumes the knowledge of the process noise covariance, and a mismatch in the process noise covariance will lead to significant error in the estimated state.

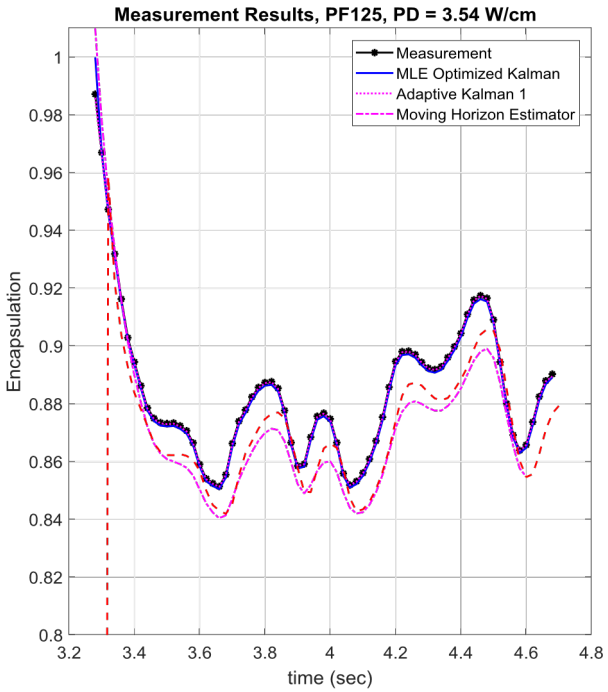

Fig. 6. Comparison of Estimators on PF125.

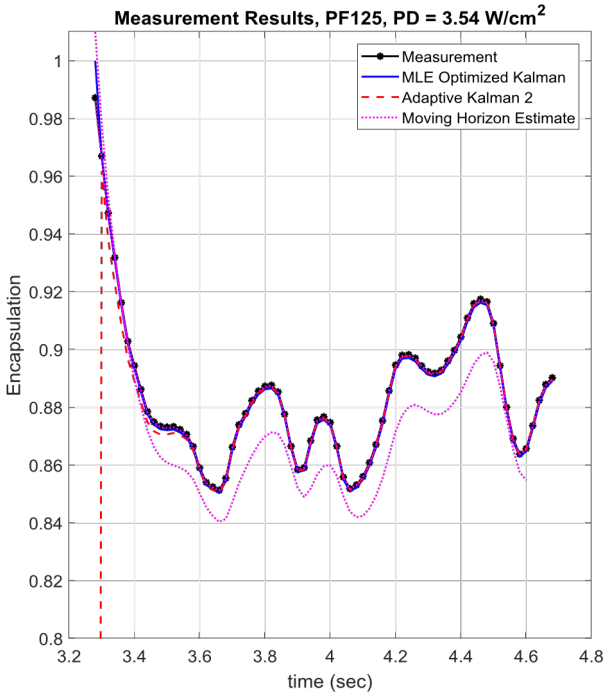

Fig. 7. Comparison of Estimators on PF125 (Tuned Adaptive Kalman).

The MHE has comparable error in estimating the percent encapsulation to the adaptive Kalman approach, and that is partially due to the fact that a window size of 5 steps was taken to decrease the computational burden of the algorithm. Further, the numerical solver was not able to make the state converge to a global minimum at all time steps.

C.Experimental Results

After validating the performance of the method in the simulation environment, the algorithms were applied to the

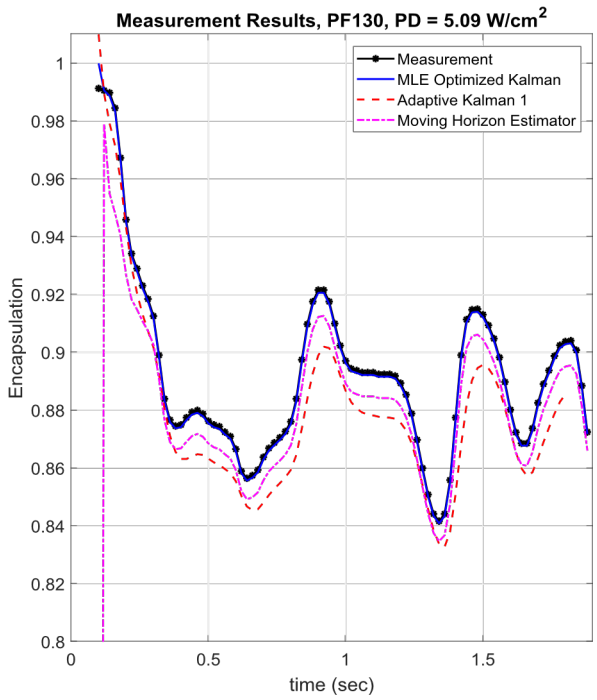

Fig. 8. Comparison of Estimators on PF130.

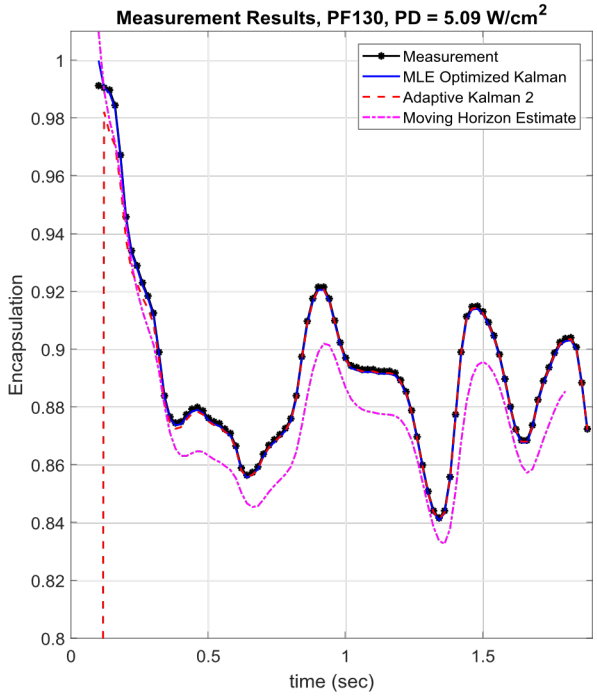

Fig. 9. Comparison of Estimators on PF130 (Tuned Adaptive Kalman).

experimental data obtained at the different ultrasonic power densities for both targeted and non-targeted micelles, given in Table I. It is worth mentioning that the adaptive Kalman filter was applied twice. First, an assumed value of the process noise covariance was used to run the algorithm. Then, a slightly tuned process noise covariance was used in the second time. Those are referred to as adaptive Kalman 1 and adaptive Kalman 2, respectively. Reasoning behind the application is to stress on the shortcomings of the adaptive

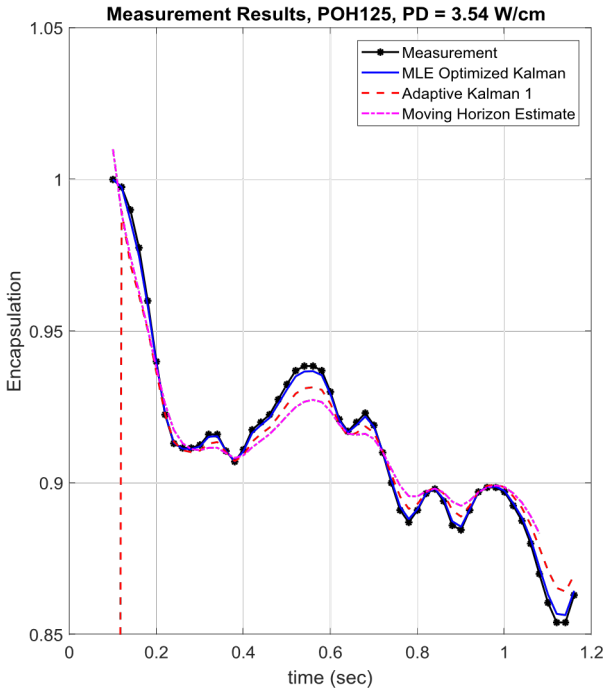

Fig. 10. Comparison of Estimators on POH125.

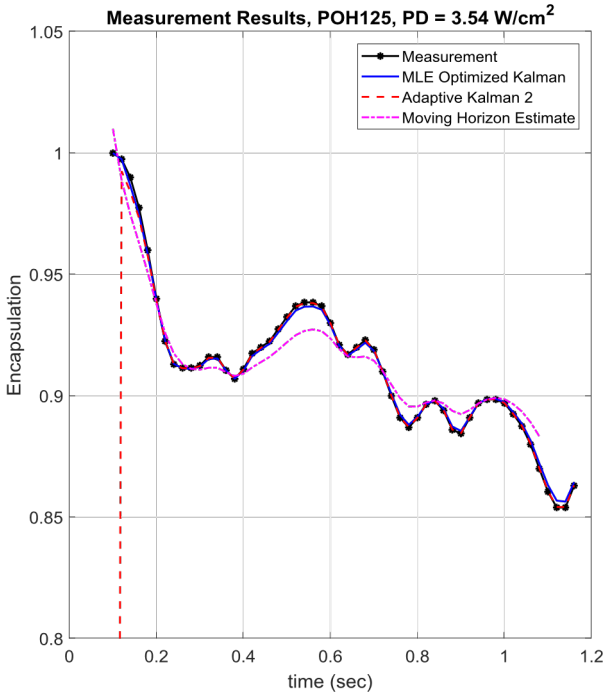

Fig. 11. Comparison of Estimators on POH125 (Tuned Adaptive Kalman).

Kalman in the sense that it only corrects for offsets in the measurement noise covariance. Figures 3, 4 and 5 present the encapsulation estimation results for the various estimators for two experimental conditions. Figures 5–11 depict the performance of the estimators when applied to the data obtained in experiments 1, 2 and 5. It can be seen that the MLE-optimized Kalman filter exhibits the best tracking

TABLE IV
ESTIMATION MEAN SQUARE ERROR OF EXPERIMENTAL MEASUREMENTS

Estimator	MSE 1	MSE 2	MSE 5
MLE Optimized Kalman Filter	$3.41\text{x}10^{-6}$	$1.58\text{x}10^{-6}$	$2.74\text{x}10^{-5}$
Adaptive Kalman Filter 1	$1.39\text{x}10^{-2}$	$1.10\text{x}10^{-2}$	$1.51\text{x}10^{-2}$
Adaptive Kalman Filter 2	$2.05\text{x}10^{-4}$	$2.24\text{x}10^{-4}$	$1.05\text{x}10^{-2}$
Moving Horizon Estimator	$1.37\text{x}10^{-2}$	$1.09\text{x}10^{-2}$	$4.49\text{x}10^{-1}$

performance of the measurements. This is closely followed by the adaptive Kalman filter 2 when the process noise covariance is tuned to a value more representative of the system dynamics. Both the adaptive Kalman filter 1 and the Moving Horizon estimation exhibit inferior performance to the aforementioned filters. This is due to the fact that the adaptive Kalman filter 1 only estimates the measurement noise statistics and assumes the dynamics noise statistics. Also, the nonlinear solver in the MHE does not always reach a solution within an acceptable time. Table IV summarizes the performance of the various algorithms presented in this paper. As discussed earlier, the MLE-optimized Kalman filter gives the smallest mean square error of the encapsulation estimates.

V. DISCUSSION AND CONCLUSION

The accurate prediction of percent re-encapsulation and hence release of chemotherapeutics from polymeric carriers is essential in the subsequent model predictive control of this novel drug delivery process. This work tackles the issue of identifying the statistics of the noise sequences affecting the dynamics and measurement of the release/re-encapsulation of the chemotherapeutic drug delivery system. After identifying the underlying uncertainty structure of the noise sequences affecting the encapsulation process and measurement, a number of estimators that are stochastic and/or optimization-based are applied to accurately estimate the drug encapsulation. The release of the drugs from the different types of micelles is modeled by a first-order differential equation. This equation is first order in drug re-encapsulation and zero-order in release.

The identification of the covariance of the dynamics and measurement noise sequences took the form of a maximum likelihood problem on this discretized system. An optimization algorithm was used to solve for the covariance values of the noise sequences. This *a priori* knowledge of the statistics of the noise sequences guarantees the optimality of the Kaman filter.

The proposed algorithms were compared against two methods available in the literature. First, an optimization based stochastic estimator, the Moving Horizon estimator, was used for comparison. Second, an adaptive Kalman filter that operates with hypothesized measurement noise covariance magnitudes was also compared to the proposed algorithm. A Monte-Carlo simulation test was carried to validate the feasibility of the estimators as the truth state is known in this environment. Subsequently, experimental validation was conducted. The MLE-optimized filters proved to outperform the other estimators. The Moving Horizon approach was

inferior to the other algorithms, because the nonlinear solver cannot converge to a good solution in a real-time application. The adaptive Kalman filter approach, while converging within a reasonable timeframe to estimate the state accurately, does not account for possible mismodeling of the dynamics noise.

REFERENCES

[1] G. A. Husseini and W. G. Pitt, "Micelles and nanoparticles for ultrasonic drug and gene delivery," *Adv. Drug Delivery Rev.*, vol. 60, pp. 1137–1152, Jun. 2008.

[2] D. G. Kanjickal and S. T. Lopina, "Modeling of drug release from polymeric delivery systems—A review," *Therapeutic Drug Carrier Syst.*, vol. 21, no. 5, pp. 345–386, 2004.

[3] V. Torchilin, "Multifunctional and stimuli-sensitive pharmaceutical nanocarriers," *Eur. J. Pharm. Biopharm.*, vol. 71, no. 3, pp. 431–444, Mar. 2009.

[4] N. Rapoport, D. A. Christensen, A. M. Kennedy, and K. H. Nam, "Cavitation properties of block copolymer stabilized phase-shift nanoemulsions used as drug carriers," *Ultrasound Med. Biol.*, vol. 36, pp. 419–429, Mar. 2010.

[5] G. A. Husseini, D. Stevenson-Abouelnasr, W. G. Pitt, K. T. Assaleh, L. O. Farahat, and J. Fahadi, "Kinetics and thermodynamics of acoustic release of doxorubicin from non-stabilized polymeric micelles," *Colloids Surf. A, Physicochem. Eng. Aspects*, vol. 359, pp. 18–24, Apr. 2010.

[6] Y. Qiu, C. Zhang, J. Tu, and D. Zhang, "Microbubble-induced sonoporation involved in ultrasound-mediated DNA transfection *in vitro* at low acoustic pressures," *J. Biomech.*, vol. 45, pp. 1339–1345, May 2012.

[7] G. A. Husseini, M. A. D. de la Rosa, E. S. Richardson, D. A. Christensen, and W. G. Pitt, "The role of cavitation in acousticallyactivated drug delivery," *J. Control Release*, vol. 107, pp. 253–261, Oct. 2005.

[8] S. Rodamporn, N. R. Harris, S. P. Beeby, R. J. Boltryk, and T. Sanchez-Elsner, "HeLa Cell Transfection Using a Novel Sonoporation System," *IEEE Trans. Biomed. Eng.*, vol. 58, no. 4, pp. 927–934, Apr. 2011.

[9] T. Siu, J. Jackson, H. Burt, and M. Chiao, "Drug uptake enhancement using sonodynamic effects at 4 MHz—A potential application for microultrasonic-transducers," *IEEE Trans. Biomed. Eng.*, vol. 54, no. 6, pp. 1153–1156, Jun. 2007.

[10] M. A. Zagrobelny and J. B. Rawlings, "Identifying the uncertainty structure using maximum likelihood estimation," in *Proc. Amer. Control Conf. (ACC)*, 2015, pp. 422–427.

[11] G. A. Husseini, F. S. Mjalli, W. G. Pitt, and N. M. Abdel-Jabbar, "Using artificial neural networks and model predictive control to optimize acoustically assisted doxorubicin release from polymeric micelles," *Technol. Cancer Res. Treat.*, vol. 8, pp. 479–488, Dec. 2009.

[12] G. A. Husseini, N. M. Abdel-Jabbar, F. S. Mjalli, and W. G. Pitt, "Modeling and sensitivity analysis of acoustic release of Doxorubicin from unstabilized pluronic P105 using an artificial neural network model," *Technol Cancer Res. Treat.*, vol. 6, pp. 49–56, Feb. 2007.

[13] G. A. Husseini, L. Kherbeck, W. G. Pitt, J. A. Hubbell, D. A. Christensen, and D. Velluto, "Kinetics of ultrasonic drug deliveryfrom targeted micelles," *J. Nanosci. Nanotechnol.*, vol. 15, no. 3, pp. 2099–2104 2015.

[14] G. A. Husseini, D. Velluto, L. Kherbeck, W. G. Pitt, J. A. Hubbell, and D. A. Christensen, "Investigating the acoustic release of doxorubicin from targeted micelles," *Colloids Surf. B, Biointerfaces*, vol. 101, pp. 153–155, Jan. 2013.

[15] J. B. Rawlings and B. R. Bakshi, "Particle filtering and moving horizon estimation," *Comput. Chem. Eng.*, vol. 30, nos. 10–12, pp. 1529–1541, Sep. 2006.

[16] M. Abdel-Hafez and G. A. Husseini, "Predicting the release of chemotherapeutics from the core of polymeric micelles using ultrasound," *IEEE Trans. Nanobiosci.*, vol. 14, no. 4, pp. 378–384, Jun. 2015.

[17] G. A. Husseini, G. D. Myrup, W. G. Pitt, D. A. Christensen, and N. Y. Rapoport, "Factors affecting acoustically triggered release of drugs from polymeric micelles," *J. Controlled Release*, vol. 69, no. 1, pp. 43–52, 2000.

[18] G. A. Husseini, N. Y. Rapoport, D. A. Christensen, J. D. Pruitt, and W. G. Pitt, "Kinetics of ultrasonic release of doxorubicin from pluronic P105 micelles," *Colloids Surf. B, Biointerfaces*, vol. 24, no. 3, pp. 253–264, 2002.

[19] C. V. Rao, J. B. Rawlings, and D. Q. Mayne, "Constrained state estimation for nonlinear discrete-time systems: Stability and moving horizon approximations," *IEEE Trans. Autom. Control*, vol. 48, no. 2, pp. 246–258, Feb. 2003.

[20] J. Rawlings, "Moving horizon estimation," in *Encyclopedia of Systems and Control*. London, U.K.: Springer, 2013, pp. 1–7.

[21] A. A. Al-Matouq and T. L. Vincent, "Multiple window moving horizon estimation," *Automatica*, vol. 53, pp. 264–274, Mar. 2015.

[22] V. Rao, J. B. Rawlings, and J. H. Lee, "Constrained linear state estimation—A moving horizon approach," *Automatica*, vol. 37, no. 10, pp. 1619–1628, 2001.

[23] C. C. Qu and J. Hahn, "Computation of arrival cost for moving horizon estimation via unscented Kalman filtering," *J. Process Control*, vol. 19, no. 2, pp. 358–363, 2009.

[24] J. Garcia-Tirado, H. Botero, and F. Angulo, "A new approach to state estimation for uncertain linear systems in a moving horizon estimation setting," *Int. J. Autom. Comput.*, vol. 13, no. 6, pp. 653–664, Feb. 2016.

[25] V. Rao and J. B. Rawlings, "Constrained process monitoring: Movinghorizon approach," *AIChE J.*, vol. 48, no. 1, pp. 97–109, 2002.

[26] P. Mohan and N. Rapoport, "Doxorubicin as a molecular nanotheranostic agent: Effect of doxorubicin encapsulation in micelles or nanoemulsions on the ultrasound-mediated intracellular delivery and nuclear trafficking," *Molecular Pharmacol.*, vol. 7, no. 6, pp. 1959–1973, Dec. 2010.